

Magnetoresistance of narrow GaAs-(Al,Ga)As heterostructures in the quasi-ballistic regime

Henk van HOUTEN, Carlo W.J. BEENAKKER, Marcel E.I. BROEKAART, Maritza G.H.J. HEIJMAN*,
Bart J. van WEES, Hans E. MOOIJ**, Jean-Pierre ANDRÉ***

On a étudié expérimentalement la magnéto-résistance en champ faible de gaz d'électrons quasi unidimensionnels dans des hétérostructures GaAs-(Al,Ga)As limitées latéralement. A basse température, les effets de taille classiques et quantiques sont importants ainsi que les effets quantiques d'interférences sur la conductivité. On a fait les expériences en régime de haute mobilité électronique, caractérisé par un libre parcours moyen élastique plus grand que la largeur de l'échantillon, mais beaucoup plus petit que sa longueur. Dans ce régime quasi balistique, le transport est balistique sur la largeur et se fait par diffusion sur la longueur. On discute les résultats expérimentaux dans le cadre des théories existantes pour ce régime.

An experimental study of the low field magnetoresistance of quasi-one dimensional electron gas channels in laterally restricted GaAs-(Al,Ga)As heterostructures is presented. At low temperatures classical and quantum mechanical size effects are important, along with quantum interference effects on the conductivity. The experiments are performed in a high mobility regime characterized by an elastic mean free path larger than the sample width, but much smaller than its length. In this quasi-ballistic regime the transport is ballistic over the width but diffusive over the length. The experimental data are discussed in relation to the available theories for this regime.

STUDIES of low temperature electronic transport in a laterally constricted two dimensional electron gas show a variety of interesting magnetoresistance effects associated with the quasi-one dimensional character of the system [1]. The effective dimensionality of a specific structure depends on the phenomenon under study, since each effect is governed by different characteristic length scales. These are the mean free path $l_c = v_F \tau_c$ (with v_F the Fermi velocity and τ_c the mean time between (elastic) collisions), the phase coherence length $l_\phi = (D\tau_\phi)^{1/2}$ (with D the diffusion constant, and τ_ϕ the phase coherence time), the thermal diffusion length $l_T = [\hbar D / (kT)]^{1/2}$ and the Fermi wavelength $\lambda_F = (2\pi/n)^{1/2}$ (with n , the sheet carrier concentration). A magnetic field introduces two additional effective length scales into the problem. Firstly, the electron trajectories become curved with the classical cyclotron orbit radius $l_{cy} = m^* v_F / (eB)$, with m^* the electron effective mass. Secondly, the effect of the field on the phase of the electron wave function is characterized by the magnetic length $l_B = [\hbar / (eB)]^{1/2}$. The magnetic field can thus serve as a probe for the length scales relevant for the effect under study.

Due to the high mobility attainable in narrow GaAs-(Al,Ga)As heterostructures the quantum interference effects such as one-dimensional weak localization and universal conductance fluctuations [2-13] are relatively large, since the characteristic diffusion lengths l_ϕ and l_T are long (of the order of 1 μm). The same holds for the quantum corrections associated with electron-electron interactions. Traditionally, one dimensional localization and interaction have been studied in evaporated metal wires or narrow silicon MOSFETs, where the mean free path is short. The existing theoretical framework [1] is derived for this *dirty metal* regime, and is not directly applicable to the *pure metal* regime of high mobility GaAs-(Al,Ga)As heterostructures, where the mean free path can exceed the sample width.

* Philips Research Laboratories 5600 JA Eindhoven (The Netherlands)

** Delft University for Technology 2628 CJ Delft (The Netherlands)

*** Laboratoire d'Electronique et de Physique appliquee (LEP) — Membre de l'Organisation de Recherche Internationale de Philips — B P 15 94451 Limeil-Brevannes Cedex (France)

In this paper we describe the *quasi-ballistic* regime defined as $W < l_e < L$ with W the channel width and L the channel length. In this regime the electrons move ballistically between the channel boundaries, but the transport is still diffusive on the length scale L . The nature of the boundary scattering will affect the diffusion constant and the various magnetoresistance effects. For simplicity we will only consider the limiting cases of diffuse and specular boundary scattering. In the quasi-ballistic regime quantum mechanical and classical size effects are both important. To study these effects we will treat the electron motion semi-classically. The validity of this approach is limited to channels wide compared to λ_F (several one dimensional subbands occupied). A study by K.K. Choi et al. [14] on wider structures down to a width of $1.1 \mu\text{m}$ has shown the onset of the quasi-ballistic size regime, while G. Timp et al. [6] and M.L. Roukes et al. [7] in recent studies have focused on narrower samples with even higher mobility, which in some sense behave as an electron waveguide. It should be pointed out that the theoretical framework for the magnetoresistance effects in the regime under study is still incomplete, so that in some cases only a qualitative discussion of the data is possible.

Two classes of magnetoresistance effects can be distinguished. *Classically* a magnetic field deflects the electron trajectories between impurity collisions (over an angle $\omega_c \tau_c$ with $\omega_c = eB/m^*$ the cyclotron frequency). In a homogeneous degenerate electron gas characterized by a single mobility μ this does not cause any magnetoresistance, since the Hall field ensures that there is no lateral drift of the electrons. In the *quasi-ballistic regime* this situation is modified by boundary scattering. In the specular case a negative magnetoresistance is observed, presumably due to the occurrence of skipping orbits [14].

Quantum Mechanically, a weak magnetic field introduces a phase shift in the electron wavefunction, depending on the electron path. A phase shift of order unity occurs for a trajectory if it encloses an area l_b^2 , with l_b the magnetic length. This affects the quantum interference corrections to the conductivity in the following way. A first quantum effect is weak localization, which is caused by constructive interference of electrons which are back-scattered after multiple elastic scattering from randomly distributed impurities. The resistivity is enhanced because of this effect. In a magnetic field trajectories enclosing a large area acquire a large phase shift. Such trajectories will, on the average, no longer contribute to the weak localization. Upon increasing the magnetic field the number of contributing trajectories will thus decrease monotonically, leading to a negative magnetoresistance. In the quasi-ballistic regime boundary scattering induces flux cancellation [13, 15], and therefore a larger field is needed to suppress weak localization. This effect is illustrated in figure 1. Also, if the mean free path is not negligibly small compared to the phase coherence length, the non-diffusive motion of the electrons on length scales short compared to the elastic length becomes important.

A second quantum interference effect is the occurrence of reproducible but aperiodic fluctuations in the

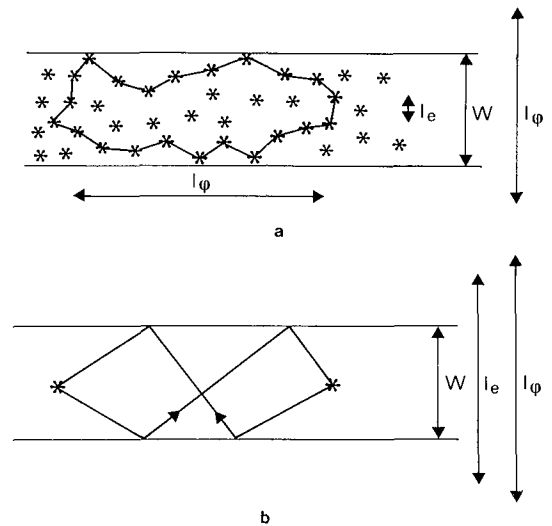


Fig. 1. Schematic illustration of the closed electron trajectories leading to 1D-weak localization in the dirty metal regime ($W \gg l_e$) (a) and in the quasi-ballistic regime ($l_e > W$) (b).

The symbol * denotes an elastic scattering event. In figure 1b, the flux piercing the closed trajectory partially cancels (the trajectory is composed of two loops of opposite orientation)

magnetoresistance, so called universal conductance fluctuations [16-18]. These fluctuations are seen in samples which are so small that their conductance is not simply determined by the average impurity concentration. Instead the *specific* distribution of the impurities over the sample is important. The fluctuations are associated with interference of the electrons moving in the random impurity potential. Even though the *pattern* of magnetoresistance fluctuations is sample specific, a correlation function can be extracted from the data, and this function can be compared with theoretical calculations for the ensemble average. The magnitude of the fluctuations is characterized by a variance, and the typical field scale on which they occur by a correlation field. The variance of these fluctuations has a universal value at absolute zero (at least if $L \gg l_e$), while at finite temperature the magnitude is reduced due to averaging and thermal smearing effects. The correlation field of the fluctuations is modified by boundary scattering in a similar way as in weak localization. Again the non-diffusive motion of the electrons on short length scales may become of importance.

A third quantum effect is the correction to the conductivity associated with electron-electron interactions. As shown by A. Houghton et al. [19] the electron-electron interaction effects on the conductivity lead to a parabolic magnetoresistance at higher fields due to the curvature of the electron trajectories. As noted by K.K. Choi et al. [14] as a consequence of boundary scattering the curvature effects will be partially suppressed in narrow channels. At present no theory for this regime is available.

At fields high enough that $\omega_c \tau \gg 1$ and $\hbar \omega_c \gg kT$ the electrons condense into Landau levels, and Shubnikov-de Haas oscillations appear in the magnetoresis-

tance. For narrow channels ($W < 2l_{\text{cycl}}, l_c$) hybrid magneto-electric subbands develop due to the lateral confinement of the electrons. The oscillations in this case show deviations from a $1/B$ periodicity. As described in detail by K.F. Berggren et al. [12, 20, 21] an analysis of this effect yields information about effective channel width and sheet carrier concentration.

We have performed an experimental study of the weak field magnetoresistance at low temperatures in GaAs-(Al,Ga)As heterostructures with effective channel widths W down to 100 nm. In earlier work [2, 9, 10, 13] we have focused on several aspects of the various magnetoresistance effects in a sample with $W \sim 110$ nm. It is the purpose of this paper to contrast the quite different behavior of the magnetoresistance of two samples with $W \sim 0.1$ and $1.1 \mu\text{m}$, and to give an overview of the great variety of magnetoresistance effects in narrow structures.

The outline of this paper is as follows. Firstly the theoretical background is outlined and the different experimental regimes are defined. Then the samples are described and the experimental results are presented. Finally a discussion of the results and concluding remarks are given.

THEORETICAL BACKGROUND

Classical effects

The classical Drude conductivity of a degenerate 2-dimensional electron gas is given by

$$\sigma_0 = n_e e^2 \tau_c / m^* = n_e e \mu,$$

with n_e the sheet carrier concentration, $\mu = e\tau_c/m^*$ the mobility and $m^* = 0.067 m_e$ the electron effective mass. Using the Einstein relation between mobility and diffusion constant this can be written as $\sigma_0 = N(E_F) e^2 D$, with $N(E_F) = m^*/(\pi \hbar^2)$ the density of states at the Fermi energy (for spin degeneracy 2, and no valley degeneracy). The diffusion constant in the absence of boundary scattering effects is $D = v_F^2 \tau_c / 2$. Specular boundary scattering does not change D from this bulk value since the electron momentum along the channel is conserved. Diffuse boundary scattering randomizes the electron momentum along the channel, leading to a reduced diffusion constant given by [13]:

$$D = \frac{1}{2} v_F^2 \tau_c \left[1 - \frac{4l_c}{\pi W} \int_0^1 s(1-s^2)^{1/2} \left(1 - \exp\left(-\frac{W}{sl_c}\right) ds \right) \right]. \quad (1)$$

In the limit $l_c/W \rightarrow \infty$, equation (1) simplifies to $D = \frac{v_F W}{\pi} \ln(l_c/W)$. However, the integral occurring in equation (1) can easily be evaluated numerically.

In the presence of a magnetic field the conductivity is a tensor quantity with components (in the absence of boundary scattering effects)

$$\sigma_{xx} = \sigma_0 / (1 + (\omega_c \tau_c)^2) \quad \text{and} \quad \sigma_{xy} = \sigma_{yx} \omega_c \tau_c,$$

with $\omega_c \tau_c = \mu B$. The measured quantities are usually the components of the resistivity tensor (which is the inverse of the conductivity tensor). The resistivity components are

$$\rho_{xx} = \sigma_{xx}^{-1} \quad \text{and} \quad \rho_{xy} = B / (n_e e).$$

In this case, there is thus no magnetoresistance, while the Hall ratio $R_H \equiv \rho_{xy}/B$ is a constant.

Boundary scattering changes this situation as mentioned earlier p. 28. K.K. Choi et al. [14] have argued that the resistance of a narrow channel with specular boundary scattering will decrease in a magnetic field because the electrons can perform skipping orbits. A saturation of this effect is expected to occur if the classical cyclotron radius $l_{\text{cycl}} = v_F / \omega_c$ becomes smaller than the channel width. Such a classical magnetoresistance effect will be independent of the temperature region where the mean free path is constant, since l_{cycl} does not depend on the temperature. A difficulty in the theoretical description is that the Hall-field is non-uniform across the channel width. Similar difficulties are encountered in the case of a thin film in parallel field with diffuse boundary scattering [22]. A preliminary investigation [23] has shown that if the non-uniformity of the Hall-field is neglected, no magnetoresistance is found in our case (because contributions of the magnetic field to σ_{xx} and σ_{xy} cancel upon inversion). In the absence of a theory*, we will here follow the qualitative considerations of K.K. Choi et al. [14].

Quantum mechanical effects

At low temperatures the classical conductivity is dominated by elastic scattering on stationary impurities. The phase coherence of the electron waves is not disturbed by such scattering events, although the phase is shifted. Inelastic scattering, on the other hand, is an example of a phase coherence limiting mechanism, setting the length scale l_ϕ . Weak localization is a consequence of constructive interference between time reversed pairs of coherently backscattered electron waves. The total backscattering probability is thereby enhanced and the conductivity is accordingly reduced. If $L \gg l_\phi \gg W$ this effect has a 1-dimen-

* In a recent paper [24] we have suggested the reduced backscattering in a magnetic field as a possible mechanism for this effect

sional character. Expressed in terms of conductance $G \equiv (W/L)\sigma$, rather than conductivity, the effect increases linearly with the ratio l_ϕ/L :

$$\delta G_{loc} = -(e^2/(\pi\hbar))l_\phi/L.$$

As discussed in [13] this standard result for the conductance change has to be modified in the case that τ_c is no longer small compared to τ_ϕ . There is no theory for this modification, but a reasonable estimate can be made if we assume that electrons can only contribute to the effect if they have at least once been scattered elastically:

$$\delta G_{loc} = -\frac{e^2}{\pi\hbar} \frac{D^{1/2}}{L} [\tau_\phi^{1/2} - (1/\tau_\phi + 1/\tau_c)^{-1/2}]. \quad (2)$$

A magnetic field destroys the constructive interference since it introduces a phase shift between the two time reversed backscattered electron waves. The effect of the magnetic field is accounted for by replacing τ_ϕ in equation (2) by the effective phase relaxation time $(1/\tau_\phi + 1/\tau_B)^{-1}$ with τ_B the magnetic phase relaxation time. In the *dirty metal* regime, defined by $l_c \ll W \ll l_\phi$, the second term between brackets in equation (2) can be neglected and the Al'tshuler-Aronov theory (AA) [25] for τ_B applies. This time is given by:

$$\tau_B = 6l_B^4/(W^2 v_F^2 \tau_c). \quad (3)$$

In the AA-theory the walls only serve to restrict the lateral diffusion, and the nature of the wall collisions is irrelevant. In the quasi-ballistic regime ($W < l_c \ll L$), however, the walls directly affect the motion of the electrons. The closed trajectories needed for the weak localization effect in this regime necessarily cross, so that as a consequence of flux cancellation the magnetic field is less effective in introducing a phase shift.

This is illustrated in figure 1. Accordingly, the time τ_B is changed. The nature of the boundary scattering (specular or diffuse) now has an influence on τ_B . For magnetic fields such that $l_B > W$ one finds [26]:

$$\tau_B = l_B^4/(K_1 W^3 v_F) + (l_B^2 \tau)/(K_2 W^2). \quad (4)$$

Here the coefficients are $K_1 = 0.11$ and $K_2 = 5/24$ for specular scattering, and $K_1 = 1/(4\pi)$ and $K_2 = 1/3$ for diffuse scattering. The theory is applicable for low fields such that $l_B > W$, which condition follows from the essential assumption that on the time scale of the phase coherence time τ_ϕ the electrons move diffusively [26].

Quantum interference also gives rise to aperiodic magnetoresistance fluctuations in small samples. At $T=0$ the amplitude of these fluctuations is independent of channel length or degree of disorder, as shown by B.L. Al'tshuler, P.A. Lee and A.D. Stone [16-18]. For this reason they are known as universal conductance fluctuations (UCF). The UCF are characterized by the correlation function:

$$F(\Delta B) \equiv \langle G(B)G(B+\Delta B) \rangle - \langle G(B) \rangle \langle G(B+\Delta B) \rangle, \quad (5)$$

where the brackets denote an ensemble average over different impurity configurations. Two characteristic quantities are the variance of the fluctuations $F(0)$ and the correlation field ΔB_c , defined by $F(\Delta B_c) = F(0)/2$. At finite temperatures the magnitude of the fluctuations is reduced as a consequence of averaging (if $l_\phi < L$) and thermal smearing (if $l_T < l_\phi, L$). In the regime $\tau_c \ll \tau_\phi$ and $W \ll l_\phi \ll L$ the variance is given by [26]:

$$F(0) = 6 \left(\frac{e^2}{2\pi\hbar} \right)^2 \left(\frac{l_\phi}{L} \right)^3 \left[1 + \frac{9}{2\pi} \left(\frac{l_\phi}{l_T} \right)^2 \right]^{-1}. \quad (6)$$

In the dirty metal regime ($l_c \ll W$) the correlation field is given by [18, 26]:

$$\Delta B_c = c_1 h/(el_\phi), \quad (7)$$

where $c_1 = 0.95$ if $l_\phi \gg l_T$ and $c_1 = 0.42$ for $l_\phi \ll l_T$. Equation (7) can be qualitatively understood, since this value for ΔB_c corresponds to a phase change of order unity for electron trajectories enclosing the largest possible coherent area Wl_ϕ . Boundary scattering will affect the correlation field as a consequence of the flux cancellation effect, just as in the case of weak localization. We will not reproduce the theoretical results for ΔB_c here, but instead refer to [26]. We note that the expression for the variance is not changed by boundary scattering, which affects only the diffusion constant. Corrections to equation (6) will be necessary if τ_c is no longer small compared to τ_ϕ . This problem is yet to be solved.

A third quantum correction to the classical Drude result for the conductivity at low temperatures is due to the effect of electron-electron interactions. The theory of this effect has recently been reviewed [1]. A discussion in relation to experiments on narrow GaAs-(Al,Ga)As heterostructures has been given by K.K. Choi et al. [14]. Under conditions also valid in our experiment the electron-electron interactions give rise to a magnetic field independent conductivity correction*. In the 1-dimensional regime $L \gg l_T \gg W$ this correction is given by:

$$\delta G_{cc} = -g_{1D} e^2 l_1 / (2^{1/2} \pi \hbar L). \quad (8)$$

Here g_{1D} is an effective interaction parameter theoretically predicted to be about 1.3 [14] for 1D-channels. The contribution of the electron-electron interactions to the conductance has a $T^{-1/2}$ dependence since $l_T \equiv (\hbar D/(kT))^{1/2}$ **.

* In the low field range where we study weak localization the magnetoresistance is an orbital effect and quantum corrections from electron-electron interactions contribute only via the so called Cooper channel [1]. Relative to the weak localization contribution this is of the order $\lambda(1 + \lambda \ln(T_F/T))^{-1} (\hbar/(k_B T \tau_\phi))^{1/2}$ where T_F is the Fermi temperature and the coupling constant λ is of order unity for GaAs [14]. For sample B ($T_F = 105$ K, $T = 4$ K $\hbar/(k_B \tau_\phi) = 1.5$ K) this would be a 10% correction which is ignored. At much higher fields where spin splitting plays a role other field dependences related to electron-electron interactions are introduced. However, at these high fields the weak localization is already completely suppressed.

** Note that in [14] l_T has been defined a factor π larger than in this paper.

do not have any effect on σ_{xx} . Admixture of classical curvature of the electron trajectories and the field independent conductivity correction δG_{cc} leads upon matrix inversion to a parabolic negative magnetoresistance [19]:

$$R(B) = G_0^{-1} + [(\omega_c \tau)^2 - 1] \delta G_{cc} / (G_0^2). \quad (9)$$

Equation (9) assumes that the electron-electron interaction correction to the conductivity is small, which is not necessarily the case for narrow channels at low temperatures. A further complication arises when boundary scattering is present, because equation (9) is based on the curvature of the electron trajectories in the bulk of the electron gas. This effect is therefore expected to be suppressed for narrow channels until the magnetic field is high enough for the electrons to be able to complete a cyclotron orbit ($2l_{cycl} < W$).

High field oscillatory magnetoresistance

The density of states $N(E)$ for a degenerate 2-dimensional electron gas does not depend on the energy E . In high magnetic fields ($\hbar\omega_c \gg kT$) Landau level quantization gives rise to states concentrated at discrete energies $(N_L + 1/2)\hbar\omega_c$. Here N_L is the Landau level index, and the degeneracy of these levels is $eB/(\pi\hbar)$ (we assume a non-resolved spin degeneracy). Shubnikov-de Haas (SdH) oscillations arise in the magnetoresistance ρ_{xx} because the density of states at the Fermi level oscillates. These oscillations are periodic in $1/B$, and from a straight line plot of N_L as a function of $1/B$ the sheet carrier concentration can be obtained according to:

$$N_L = n_s \pi \hbar / (eB). \quad (10)$$

In narrow channels deviations from this behavior occur, because the density of states is altered due to size quantization. The detailed shape of the lateral confining potential determines the positions of the 1-dimensional subbands. In a quantizing magnetic field hybrid magneto-electric subbands develop. For a detailed treatment of this subject we refer to K.F. Berggren et al. [20, 21]. A quantum mechanical analog of the classical cyclotron radius l_{cycl} can be defined:

$$l_{cycl}^{qm} = [\hbar(2N_L + 1) / (m^* \omega_c)]^{1/2}. \quad (11)$$

For high magnetic fields, where $l_{cycl}^{qm} < W/2$ the electrons can complete cyclotron orbits within the channel, and the density of states becomes similar to that of a 2-dimensional electron gas with Landau-level quantization. From the high field slope of a straight line plot of N_L as a function of $1/B$ the sheet carrier concentration can be estimated according to equation (10). Deviations from a straight line start at $l_{cycl}^{qm} \sim W/2$. From this simple criterion an estimate for the channel width can be obtained.

EXPERIMENTAL RESULTS

Samples

The samples have been fabricated on moderately high mobility ($10 \text{ m}^2 \cdot \text{V}^{-1} \cdot \text{s}^{-1}$ at low temperatures) GaAs-Al_xGa_{1-x}As heterostructure material, grown by metal-organic chemical vapor deposition ($x = 0.35$). The sheet carrier concentration in this material (when cooled in the dark) was $5 \times 10^{15} \text{ m}^{-2}$. The fabrication technology is illustrated in figure 2. Long, narrow channels connecting broad 2-dimensional electron

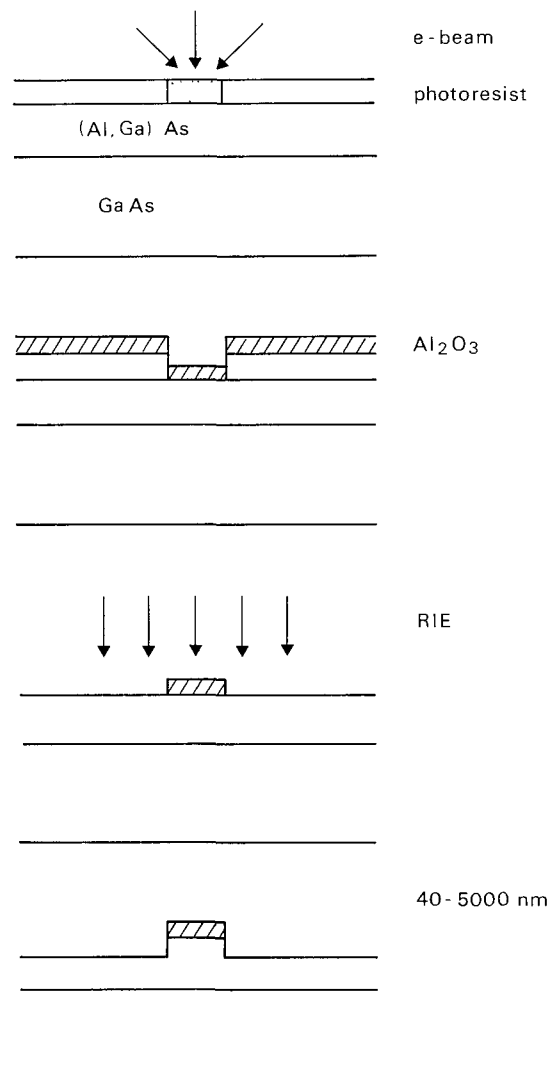


Fig. 2. Main fabrication steps for the shallow mesa etch definition of the narrow electron gas channel in a GaAs-(Al,Ga)As heterostructure.

The Al₂O₃ pattern, which serves as etch mask during subsequent anisotropic etching (Reactive Ion Etching, RIE), is defined by electron beam lithography.

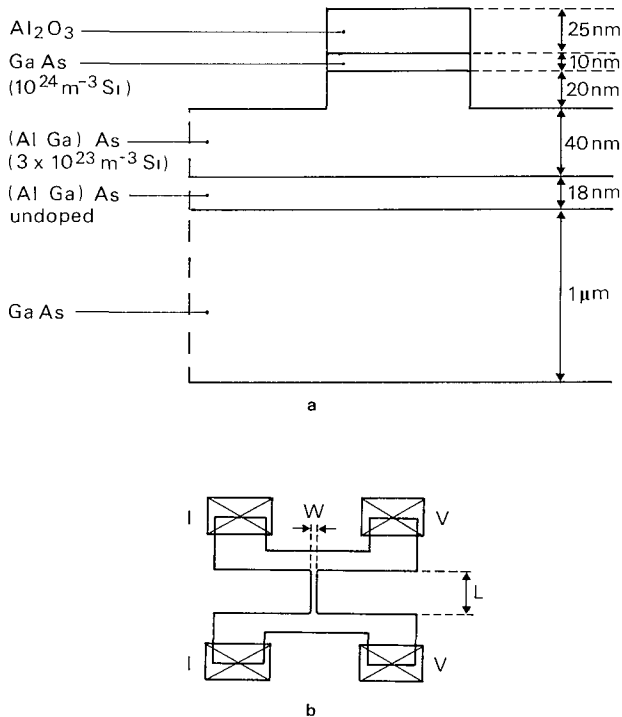


Fig. 3. Schematic cross section of the shallow mesa etched GaAs-(Al,Ga)As heterostructure **(a)** and layout of the devices **(b)**.

- a** a conducting electron layer, narrower than the mesa width, is formed at the lower GaAs (Al,Ga)As interface
b a narrow channel of width W and length L connects two broad two dimensional electron gas regions, provided with two ohmic contacts each

gas regions with two ohmic contacts each have been defined using electron-beam lithography and reactive ion etching. Further details on the fabrication process have been given elsewhere [2]. In figure 3 a schematic cross section and geometry of the structure are shown. An essential feature is that, as a consequence of a shallow mesa channel definition, the electron gas is laterally confined by a smooth depletion potential. This prevents degradation of the channel mobility by scattering from rough surfaces, or from the presence of electron traps on the sidewalls. The effective channel width can be appreciably less than the lithographic width, and also the sheet carrier concentration will be lower than in wide channels. We note that in the sample geometry (fig. 3) four terminal measurements eliminate contributions from contact resistances or from admixture of the Hall-effect. In the case $l_e \gg W$, however, a Sharvin constriction [27] resistance of order $\rho l_e / W$ is measured in series with the channel resistance. The relative error is thus of order l_e / L , which in our case is a few percent. For higher mobility channels this problem would be much more serious, necessitating longer channels.

A series of samples with lithographic width between $8 \mu\text{m}$ and $0.5 \mu\text{m}$ have been studied. In this paper we will focus on two samples : sample A with lithographic width $1.5 \mu\text{m}$ and sample B with lithographic width $0.5 \mu\text{m}$. Both channels are $10 \mu\text{m}$ long. The elastic mean free path in the wide regions is $l_e \sim 1 \mu\text{m}$.

As we will show below, sample A is slightly wider than l_e , while sample B is fully in the quasi-ballistic regime. The magnetoresistance of both samples is qualitatively quite different. We will first give an overview of the results, and subsequently we will give a detailed discussion.

In order to get some feeling for the influence of the channel width on the transport properties we have plotted in figure 4 the channel resistance, multiplied by W^{th}/L . For comparison the resistivity of a wide channel is also plotted. It is clear from figure 4 that the *real* channel width in the case of narrow channels is smaller than the lithographic width. This is confirmed by the fact that channels with W^{th} smaller than about 400 nm turned out to be insulating. The lateral depletion width for our fabrication process is thus about 200 nm on each side of the channel. (According to M.L. Roukes et al. [7] it is possible to reduce this effect by optimizing the etch depth). It should be noted that even in the simple case of specular scattering (which will be shown to apply to our samples) the mobility of the narrow electron gas channels depends on the channel width in an indirect way : the sheet carrier concentration diminishes on reducing the width. The mobility in heterostructures at low temperatures is dominated by ionized impurity scattering. In these systems the mobility is known to be proportional to $n_s^{3/2}$. In table I it is shown for the channels studied that the ratio of μ and $n_s^{3/2}$ is indeed nearly constant. It can thus be concluded that the mobility in our samples is not significantly degraded in the course of the microfabrication process*. We will return to the problem of determining the real channel width later. The large resistance rise at low temperatures for sample B is related to quasi-one dimensional weak localization and electron-electron interaction effects. Part of the resistance increase on lowering the channel width is related to the lower value for n_s , and thus for μ . We note that the sheet carrier concentration varies

* The same conclusion was reached by H Z Zheng et al [4] in their study of narrow channels defined by a split-gate technique

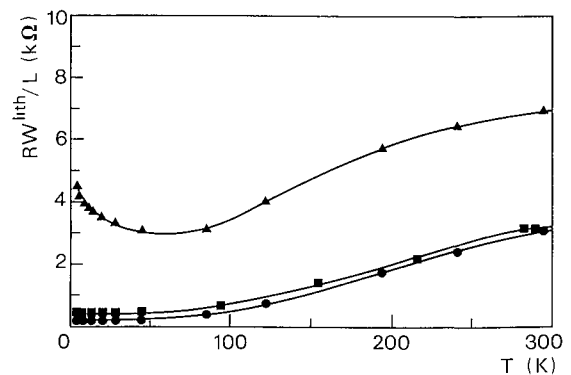


Fig. 4. Temperature dependence of the channel resistance R (multiplied by W^{th}/L) for sample A (■), sample B (▲) and for a wide channel (●)

From [2]

TABLE I
Parameters for a wide channel and for samples A and B.

sample	$W^{\text{ lith}}$ (μm)	W (μm)	n_s (10^{15}m^{-2})	μ ($\text{m}^2 \cdot \text{V}^{-1} \cdot \text{s}^{-1}$)	$\mu/n_s^{3/2}$ ($10^{-23}\text{m}^5 \cdot \text{V}^{-1} \cdot \text{s}^{-1}$)	l_e (μm)	l_p (1 K) (μm)	l_t (1 K) (μm)
wide			4.0	10	3.9	1.0		
A	1.5	1.1	3.6	7.5	3.5	0.74		0.85
B	0.5	0.12	2.5	4	3.2	0.35	0.87	0.54

somewhat (up to 20 %) each time the sample is cooled down from room temperature. This should be kept in mind if different data-sets for the same sample are to be compared. No drift has been observed if the samples were kept at low temperatures, however.

In figure 5 and 6 the magnetoresistance for samples A and B are shown in the temperature region between 4 K and 28 K. The behavior of sample A, which has a lithographic width of 1.5 μm , is similar to the results reported by K.K. Choi et al. [14] for a sample with $W^{\text{ lith}} = 1.9 \mu\text{m}$, $L = 6.2 \mu\text{m}$. A practically temperature independent negative magnetoresistance is observed around $B = 0 \text{ T}$. We attribute this to the classical skipping orbit effect of [14]. For higher fields a parabolic temperature dependent negative magnetoresistance occurs as predicted by equation (9), and the onset of Shubnikov-de Haas oscillations is seen. On increasing the temperature this negative magnetoresistance is reduced, and eventually a positive magnetoresistance is seen at high temperatures.

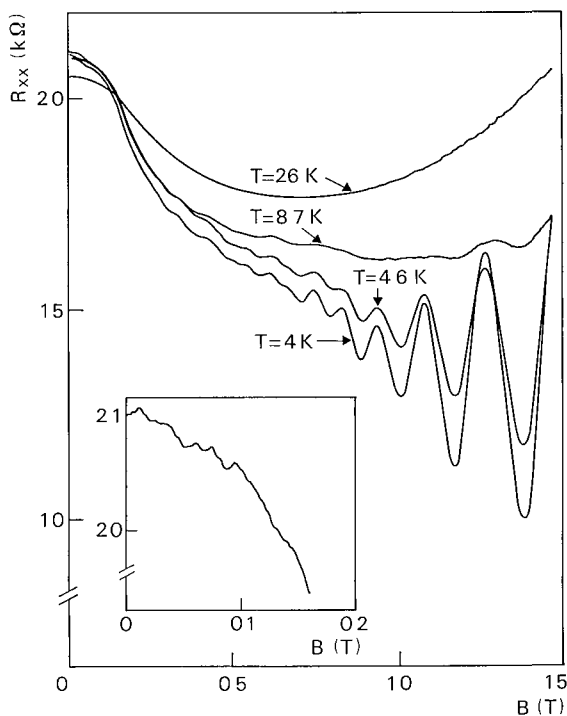


Fig. 5. Magnetoresistance for sample A. The inset shows reproducible fluctuations at 4 K.

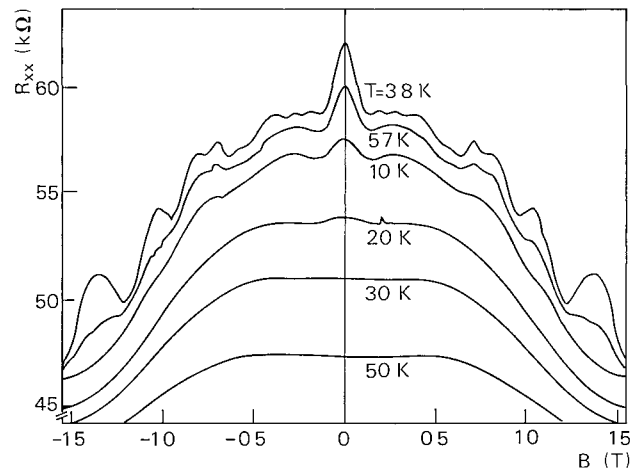


Fig. 6. Magnetoresistance for sample B.

From [2]

The magnetoresistance of the narrower sample B (fig. 6) looks very different. This behavior arises because the quantum mechanical corrections to the conductivity are much larger in this sample, while the classical skipping orbit effect occurs at a much higher field scale, so that it can only be seen clearly at higher temperatures where the quantum mechanical effects are suppressed. A pronounced, temperature dependent, negative magnetoresistance peak is seen around $B = 0 \text{ T}$, which we attribute to weak localization in the quasi-ballistic regime. The temperature dependent parabolic negative magnetoresistance seen at higher fields in sample A appears to be suppressed in the narrow channel B. Large aperiodic fluctuations in the magnetoresistance occur at lower temperatures, while Shubnikov-de Haas oscillations begin to appear around 1 T (see p. 36). All magnetoresistance effects in the present field range are caused by the orbital movement of the electrons in the plane of the original 2-dimensional electron gas. This is illustrated in figure 7, where the angular dependence of the magnetoresistance is shown for this sample (the conductance fluctuations follow a different pattern than in figure 5 because the sample had been cycled to 293 K). The minima of the fluctuations shift with $\cos\theta$ (not shown), which confirms again that they are sensitive to the perpendicular component of the field only. We now turn to a more detailed discussion of the various phenomena.

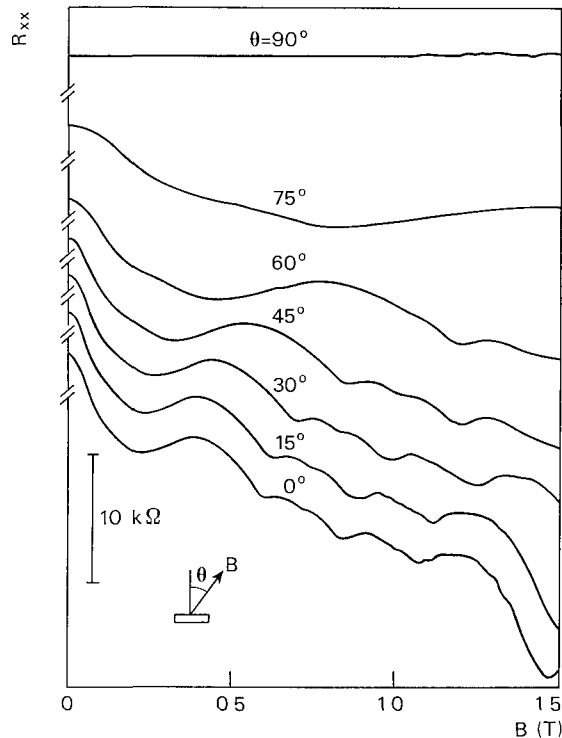


Fig. 7. Angular dependence of the magnetoresistance for sample B at 4 K

From [9]

Classical skipping orbit effect

The temperature independent negative magnetoresistance seen in figure 5 for sample A has a half-width at a field ~ 0.2 T and in figure 6 for sample B at ~ 1 T. This is consistent with the classical skipping orbit effect discussed p. 29. The interpretation leads to values for the respective channel widths of $1.0 \mu\text{m}$ and $0.15 \mu\text{m}$. These values are in reasonable agreement with other estimates (see table I).

Weak localization

We have measured the negative weak field ($B < 0.2$ T) magnetoresistance for sample B for temperatures between 100 mK and 14.3 K. Representative data between 4 K and 14 K are plotted in terms of conductance in figure 8. The observed effect is clearly a 1-dimensional weak localization effect, since the 2-D weak localization theory would predict a saturation of the effect if the magnetic length $l_b = [\hbar/(eB)]^{1/2}$ becomes comparable to l_c , which implies much lower saturation fields than the typically observed fields of 0.2 T. Although the AA-theory (see p. 29) for 1-D weak localization fits our data well, this analysis is *inconsistent* since the resulting parameter values ($W \sim 60$ nm, $l_c \sim 600$ nm) violate the criterion $l_c \ll W$ for its applicability.

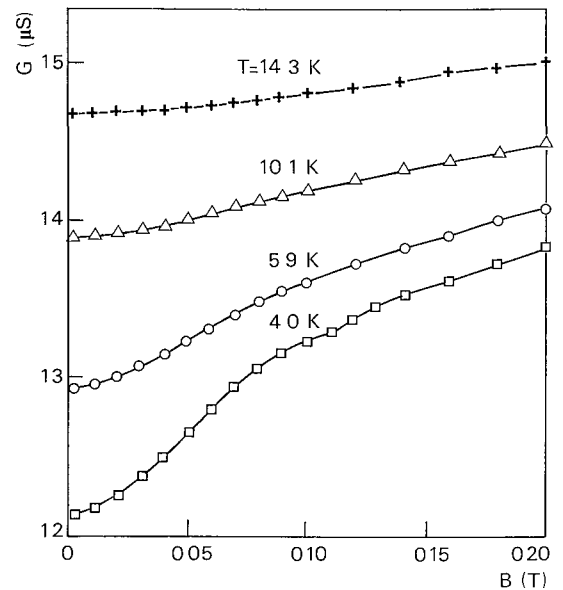


Fig. 8. Magnetoconductance for sample B caused by weak localization

Lines are to guide the eye

From [10]

The data are analyzed in terms of the equations given pp. 30-31 [10]. The electron gas density in the narrow channel is estimated to be $2.5 \times 10^{15} \text{m}^{-2}$ (see p. 36). Two of the three unknown parameters (W , τ_c and τ_ϕ) can be eliminated using estimated values for the classical conductance ($G_0 = [m^* e^2 / (\pi \hbar^2)] (W/L) D = 18 \times 10^{-6} \text{S}$, as obtained from extrapolation of a plot of $G(0)$ versus $T^{-1/2}$, see figure 11) and for the saturation value of the magnetoconductance :

$$G(\infty) - G(0) = \frac{e^2}{\pi \hbar} \frac{D^{1/2}}{L} \left(\tau_\phi^{1/2} - \left(\frac{1}{\tau_\phi} + \frac{1}{\tau_c} \right)^{-1/2} \right). \quad (12)$$

The third parameter is obtained by a fit, considering only data points for which $l_b > W$ (see p. 30). This procedure was followed for the 4.0 K data, for which we estimate $G(\infty) = 13.9 \times 10^{-6} \text{S}$. Despite the uncertainties in $G(\infty)$ we did not perform a two or three parameter fit, because of the limited field range ($l_b > W$) available for the fit. For fits to the data at other temperatures the values for W and l_c were kept fixed. As shown in figure 9, for specular scattering a reasonable fit is obtained with $W = 106$ nm, $l_c \equiv v_F \tau_c = 351$ nm. (An assumption of diffuse scattering does not work since it leads to values for l_c much larger than in wide 2DEG regions, which is evidently unreasonable). We will refrain from a detailed discussion of the values for l_ϕ given in figure 9, since in view of the uncertainties in the modelling of the short time behavior (in equation (2)) these values may not be very accurate. Finally, we remark that at millikelvin temperatures the weak localization effect (and also corrections to the conductivity due to electron-electron interactions) are so large that they are no longer a small correction to the Drude conductivity. The

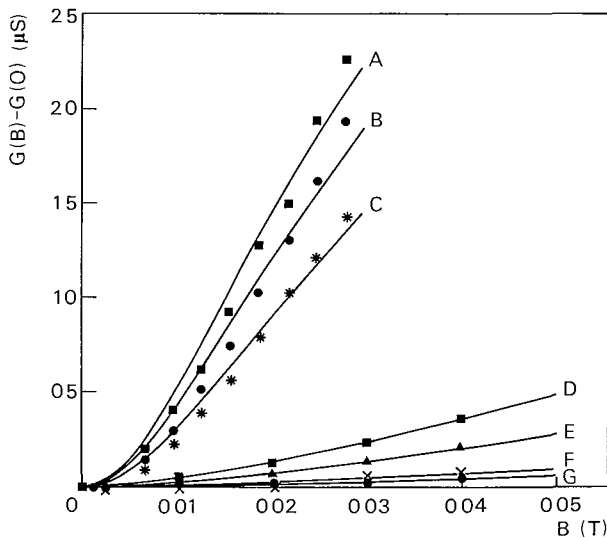


Fig. 9. Magnetoresistance data between 500 mK and 14.3 K for sample B

The solid curves result from the theory for weak localization in the quasi-ballistic regime with specular boundary scattering

From [10]

A $T=0.5$ K, $l_{\phi}=1038$ nm, B $T=0.7$ K, $l_{\phi}=970$ nm, C $T=1$ K, $l_{\phi}=869$ nm, D $T=4$ K, $l_{\phi}=450$ nm, E $T=5.9$ K, $l_{\phi}=375$ nm, F $T=10.1$ K, $l_{\phi}=243$ nm, G $T=14.3$ K, $l_{\phi}=213$ nm

various conductivity corrections presumably are no longer additive in this case (see equation (13) and also figure 11). This may be the reason that at temperatures below 200 mK a saturation is found of the values for l_{ϕ} obtained from the weak localization in the present analysis.

Universal conductance fluctuations

We now turn to the fluctuations observed in the magnetoresistance at lower fields (see figures 5 and 6). As expected from the UCF theory the oscillations in sample A are smaller than those in sample B, and they occur on a smaller typical field scale, as a consequence of the larger width. (The width ratio of about 10 roughly corresponds to the field scale ratio; cf. equation (7)). We will limit the quantitative discussion to sample B [26]. For a comparison with the theoretical predictions the correlation field and variance have to be extracted from the data. Under the usual ergodic hypothesis [18] the average over impurity configurations in equation (5) is replaced by an average over B after a correction for a constant trend which would give rise to spurious correlations. In figure 10 the resulting correlation function for a magnetoconductance trace at 2.4 K is shown. We find $F=1.9 \times 10^{-4} [e^2/(2\pi\hbar)]^2$ and $\Delta B_c=0.05$ T, with an estimated error of 30%. From equation (6), with an estimated value for W , we thus find $l_{\phi} \sim 500$ nm, which compares reasonably well with the weak localization result (600 nm). The predicted ΔB_c , however, is a factor of two higher than the measured quantity. This discrepancy seems

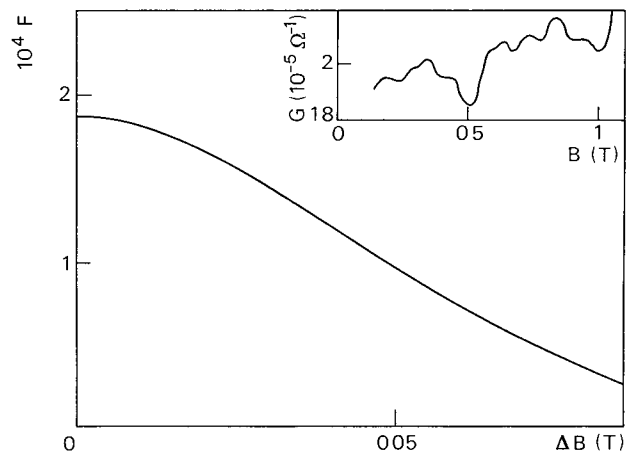


Fig. 10. Correlation function F , in units $(e^2/(2\pi\hbar))^2$ obtained from the magnetoresistance measurements for sample B at 2.4 K.

From [9]

The inset shows the conductance fluctuations, from [23]

rather large to attribute entirely to uncertainties in W . More likely, the reason that the correlation field turns out smaller than predicted is that, as we increase the field increment ΔB , more and more electrons lose phase coherence before entering the regime of diffusive motion. This breakdown of coherent diffusion is beyond the UCF theory, but it certainly plays a role in systems where τ_{ϕ} is of the order of the elastic scattering time. The effect of flux cancellation on the correlation field [25] can be studied without these complications in systems with $l_c > W$ but $\tau_{\phi} \gg \tau_e$.

Electron-electron interaction effects

The zero field conductance is given by :

$$G(0) = G_0 + \delta G_{loc} + \delta G_{ee}. \quad (13)$$

The negative localization and electron-electron interaction corrections have been given in equations (2) and (8). Once δG_{loc} is known, δG_{ee} follows from equation (13). This is illustrated for sample B in figure 11 (only low temperature data points are considered for which the short time corrections in the weak localization analysis are relatively unimportant). The resulting values for δG_{ee} are seen to be proportional to $T^{-1/2}$, as predicted by equation (8), while they also extrapolate to the correct value for G_0 . If we use $D=0.039$ m²·s⁻¹ we find from the slope $g_{1D}=1.5$, which nicely agrees with the theoretical value (1.3). The absence of the parabolic negative magnetoresistance of equation (9) is presumably caused by a quenching of the classical curvature of the electron trajectories by boundary scattering [14].

For sample A the relative effect $\delta G_{loc}/G_0$ is very small, and also the sample is only marginally 1-dimensional,

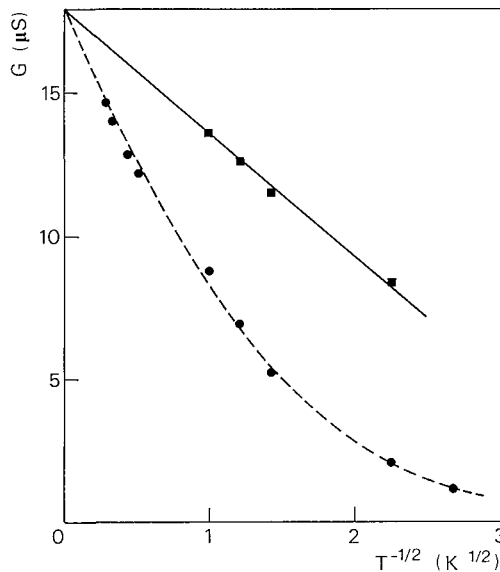


Fig. 11. Zero field conductance (●) and conductance corrected for the weak localization contribution (■) for sample B as a function of $T^{-1/2}$

The straight line reflects the temperature dependence for the electron electron interaction effect predicted by equation (8). The extrapolated value at high temperatures is the classical part of the conductance G_0 .

so that the preceding analysis cannot be done. A negative parabolic magnetoresistance associated with electron-electron interactions (equation (9)) does appear to be present in figure 6, but because boundary scattering still plays a substantial role a reliable quantitative analysis is not yet possible for this sample (a simple estimate using $g_{1D} = 1.5$ does give the correct order of magnitude). The positive parabolic magnetoresistance which is seen in figure 6 at higher temperatures (20 K) is attributed to the effect of a non-fully degenerate electron gas, leading to a classical magnetoresistance associated with an energy dependent relaxation time.

High field oscillatory magnetoresistance

In sufficiently high magnetic fields (depending on the sample width) Shubnikov-de Haas (SdH) oscillations appear in the magnetoresistance, as is already apparent in figure 5. The carrier concentration resulting from the linear part of the corresponding Landau level index plot at high fields is given in table I. At lower fields deviations from linearity occur, although it is difficult to discriminate between UCF and density of states effects in this field region. We do not reproduce the relevant figures here but instead refer to [9, 21]. For sample B a clear deviation from linearity is seen, and an estimate for the channel width of 110 nm is obtained according to equation (8).

As described elsewhere [9, 21], a more sophisticated analysis is possible if a parabolic potential is assumed for the lateral confinement of the electrons. Again an estimate for the width is found ($W \sim 138$ nm), which

agrees fairly well with the estimate given above, and with the width derived from weak localization or from a simple constant depletion width argument.

DISCUSSION

In the preceding section we have tried to show that the samples under study have a rich magnetoresistance behavior at low temperatures. Not all of the effects are quantitatively understood. Still, a qualitative understanding of the various phenomena has been reached, which can serve as a guideline towards future experiments. The weak localization in the quasi-ballistic regime is relatively well understood. It would be rather premature, however, to perform a detailed analysis of the resulting 1D-coherence time in terms of the various proposed phase breaking mechanisms [28], mainly due to the uncertainties in the modelling of the short time corrections in equation (2).

A perennial problem in the study of transport in quasi-one dimensional electron gas channels in semiconductor structures is that one of the key parameters, the channel width, is not known. We have discussed the various ways in which this width can be extracted from the experimental data, and consistent results are obtained. As summarized in table I, large sidewall depletion effects are found. Similar conclusions have been reached by other authors [5, 6]. It would be interesting to compare these findings with self-consistent solutions of the electrostatic confinement, although the proper modelling of the boundary conditions on the exposed surfaces presents a problem [29]. In the quasi-ballistic regime ($l_e > W$) boundary scattering affects the various magnetoresistance mechanisms. We have found that in our channels the boundary scattering is predominantly specular. This can be understood as a consequence of the large Fermi-wavelength ($\lambda_F \sim 40$ nm). Specular scattering occurs for wavelengths larger than the scale of the surface irregularities.

We conclude by indicating some experimental and theoretical directions in which the present study could be extended. Further experimental work will be needed to investigate the role of the sample length L . A study of the transition from diffusive to ballistic electron motion could thus be envisaged. Here we would like to point out that a further increase of the mobility (e.g. by use of material grown by molecular beam epitaxy) will lead to an increase in l_e and l_T . At the same time, however, the electron motion will increasingly become ballistic. Disorder related phenomena such as weak localization and universal conductance fluctuations may thus disappear for such extremely high mobility channels. On the other hand, 1D-subband related effects will become impor-

- 27 SHARVIN (Y V) — **A possible method for studying Fermi surfaces.** Zh Eksp & Teor Fiz, **48**, (1965), 984-985 Sov Phys-JETP, **21**, (1965), 655-656
- 28 ALTSHULER (B L), ARONOV (A G), KHMELNITSKII (D E) — **Suppression of the localization effects by high frequency fields and the Nyquist noise.** Solid State Commun, **39**, (1981), 619-623
- 29a LAUX (S E), FRANK (D J), STERN (F) — **Quasi-one-dimensional electron states in a split-gate GaAs-AlGaAs heterostructure.** Proc 7th Int Conf on Electronic Properties of Two-Dimensional Systems, Santa Fe, (1987) Surf Sci, **196**, (1988), 101-106
- 29b STERN (F) — Private communication
- 30 VAN WEES (B J), VAN HOUTEN (H), BEENAKER (C W J), WILLIAMSON (J G), KOUWENHOVEN (L P), VAN DER MARELAND (D), FOXON (C T) — **Quantized conductance of point contacts in a two-dimensional electron gas.** Phys Rev Lett, **60**, (1988), 848-850
- 31 WHARAM (D A), THORNTON (T J), NEWBURY (R), PEPPER (M), AHMED (H), FROST (J E F), HASKO (D G), PEACOCK (D C), RITCHIE (D A), JONES (G A C) — **One-dimensional transport and the quantization of the ballistic resistance.** J Phys C, **21**, (1988), L209-L214
- 32 TESANOVIC (Z), JARIC (M V), MAEKAWA (S) — **Quantum transport and surface scattering.** Phys Rev Lett, **57**, (1986), 2760-2763
- 33a LANDAUER (R) — **Spatial variation of currents and fields due to localized scatterers in metallic conduction.** IBM J Res & Dev, **1**, (1957), 223-231
- 33b LANDAUER (R) — **Electrical transport in open and closed systems.** Z Phys B, **68**, (1987), 217-228
- 34 CHAKRAVARTY (S), SCHMID (A) — **Weak localization: the quasi-classical theory of electrons in a random potential.** Phys Rep, **140**, (1986), 193-236